An Environmental Justice Lens for Measuring Neighborhood Scale Vulnerability

An exploratory analysis by
Nagendra Singh, Joe Tuccillo, Christa Brelsford,
Taylor Hauser, and Sujithkumar Surendrannair

CLIMATE CHANGE SCIENCE INSTITUTE
OAK RIDGE NATIONAL LABORATORY

An Environmental Justice Lens for Measuring Neighborhood Scale Vulnerability

Team: Nagendra Singh, Joe Tuccillo, Christa Brelsford, Taylor Hauser, Sujithkumar Surendrannair

Introduction

Environmental justice [1,2,3] is a key aspect of the federal government's strategy for managing the adverse impacts of climate change. Nevertheless, we do not currently have robust tools for projecting the differential socio-economic risks of future adverse events. Simpson et al [4] highlight one framework for describing climate change risk as a combined function of hazard, vulnerability, exposure, and response (Figure 1) and build on this framework of risk to characterize. There is extensive literature from the climate community characterizing potential future climate hazards. However, understanding future climate risks and their environmental justice consequences also requires assessing future vulnerability, exposure, and responses.

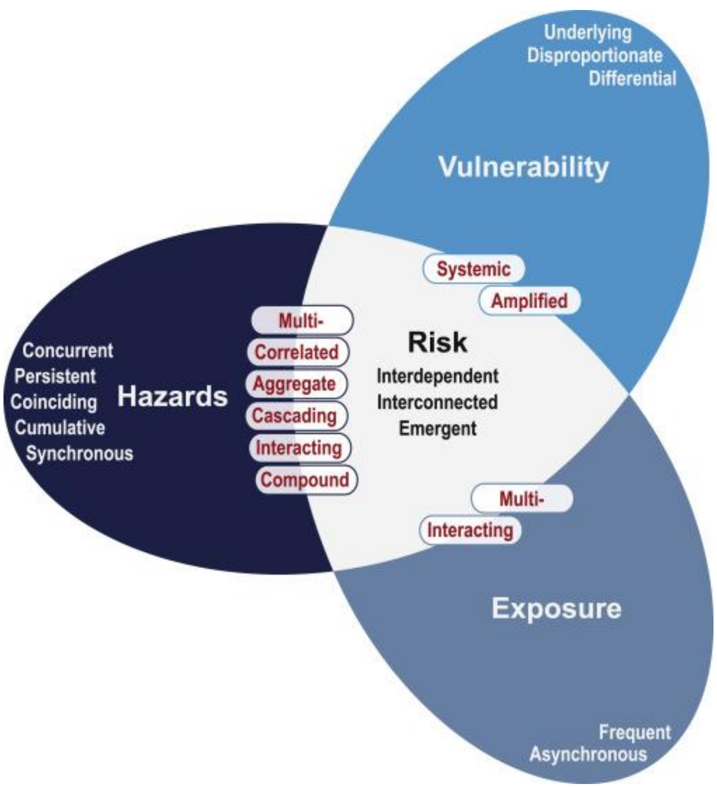

Figure 1: Reproduced from [Simpson et al.]. This figure highlights the diversity of complex climate change risk terminology.

ORNL has long-standing expertise in measuring contemporary populations and analyzing those at risk in contemporary adverse events [5]. We are actively expanding our expertise assessing present-day vulnerable populations [6]. However, these population and demographic tools have not been connected to the broader DOE climate research community, and DOE has not invested significantly in this type of socio-demographic consequence assessment. Compared to the level of effort expended in modeling the climate system, investment in impacts, adaptation, and vulnerability (IAV) is small, and the impacts of extreme climate events are only rarely assessed from the perspective of disproportionate harm.

Some integrated assessment models (IAMS) have tried to quantify economic risks of climate change [7], but this is not yet sufficient to assess how impacts vary across socio-economic and demographic groups. Vulnerability assessments have become increasingly available at the scale of neighborhoods [8, 9, 10], but a persistent problem is their lack of attention to individual-level drivers of socio-economic impacts from hazards. Neighborhood-level vulnerability indicators often consist of aggregate population characteristics that overlook how specific people could be affected by a damaging event. It remains critical to account for individual context in vulnerability assessments, as the experiences and interactions of people within a neighborhood underpin the collective capacity to cope and recover from hazards [11]. For example, while everyone in low-lying neighborhoods in New Orleans was vulnerable to Hurricane Katrina, those without access to a vehicle faced substantially greater impediments to evacuation and eventual recovery [12]. This convergence of locational and situational vulnerability had a dramatic impact on the ability of these residents, and the neighborhoods they lived in, to recover from the hurricane's aftermath. Measuring the linkages between individual and neighborhood-level risk enables a fuller understanding of disproportionate impacts of climate stressors like extreme heat events [13,14], providing a means to ensure that adaptation strategies promote social equity.

Background

The magnitude and location of population exposed to extreme events and climate hazards has typically been estimated by using socioeconomic indices based on census geographies. For example, Cutter et al. [15, 16] used socio-economic indicators to identify counties which were relatively at higher risk of impacts from natural hazards, which has in turn been adapted by the Centers for Disease Control [17] and the US Environmental Protection Agency [18] to identify various census geographies at risk. However, these approaches do not capture the variability of vulnerabilities within these geographic areas, nor are they flexible enough for elucidating distributional aspects of a neighborhood's risk from current and future climate hazards. They also lack information on differential vulnerability across neighborhoods and social groups: This is essential to understanding the equity and environmental justice impacts of climate change. To ensure that social equity and environmental justice consequences can be fully incorporated into current and future climate impact assessments, we need to understand what influences the resilience of a specific neighborhood population to extreme events in terms of hazard, vulnerability, and adaptive capacity.

Methods

In this exploratory analysis, we have partially developed a methodology to downscale current and future climate change risk at neighborhood scale by estimating vulnerability and adaptive capacity of the neighborhood. We use techniques to delineate 'neighborhoods-at-risk' over the landscape in terms of factors contributing to the vulnerability and adaptive capacity of neighborhoods. These methods are not constrained by census boundaries such as counties and block groups. This flexible approach for geographic delineation can also be applied to future urban morphologies to assist in the projection of high-risk neighborhoods. We use populations derived from census microdata to disaggregate factors linked to social and economic inequality, enabling us to identify the drivers of vulnerability within and across neighborhoods and to classify neighborhoods based these drivers. Once such 'neighborhoods-at-risk' over the landscape have been identified, we can establish scenarios and explore the distributional impact of projected climate change effects in the future. These, 'neighborhoods-at-risk' can be used as an operational unit of risk over the landscape to evaluate the environmental justice consequences of current and future climate hazards.

We are exploring strategies to measure the environmental justice consequences of climate change in the Atlanta Metropolitan Statistical Area (MSA). We characterized neighborhoods in Atlanta by common sets of built environment and socio-economic characteristics, using two distinct steps. In step one, we differentiated neighborhoods by using machine learning to cluster building outlines derived from high resolution satellite imagery. In step two, we used populations derived from the Public Use Microdata Sample (PUMS) to disaggregate socio-economic factors like race, age, sex, poverty status, and housing through maximum entropy dasymetric modeling. This enables us to classify neighborhoods based on vulnerabilities shared among their residents. We then apply our neighborhood typology to evaluate differential impacts across socio-economic groups due to urban heat island (UHI) and climate-driven extreme heat events (EHEs).

1. Neighborhood Delineation Using Clustering of Building Outlines

We used approximately 1.63 million structures within the Atlanta MSA for our analysis. A total of 21 features were calculated for each structure for classification. Broadly, these features consist of four categories: geometric, engineered, ancillary, and contextual. These features were analyzed by a supervised binary residential classifier. This model classifies each structure as either residential or nonresidential. The residential structures were kept for further processing. Lastly, an unsupervised clustering algorithm (DBSCAN) was used to cluster structure centroids into groups that form the basis of our residential 'neighborhoods'.

DBSCAN was run with various iterations of the two parameters, epsilon and minimum samples. Epsilon is the radius of a neighborhood that is considered for each object. Minimum samples describe the threshold density for a core object or potential center of a cluster. Because appropriate parameters for DBSCAN related to structures detections was unknown, the algorithm was run multiple times with various iterations of parameters. The results where Epsilon = 100 and Minimum samples = 10 were chosen for analysis. These results were chosen because they visually aligned with the desired results of the modeler. Additionally, compared to the other iterations it produced a high number of consistent neighborhoods with only a few large runaway cluster neighborhoods.

These neighborhood measures were then used as inputs to a K-Means unsupervised clustering algorithm.

2. Neighborhood Delineation Using Geodemographic Classification

Geodemographics broadly involves the study of spatial heterogeneity in the social properties of communities across urban systems [19]. Widely applied to aid urban planning and public service delivery [20], geodemographics provides a useful, but frequently overlooked lens through which to identify potentially underserved populations within urban neighborhoods with respect to environmental justice concerns [21] and climate stressors, including urban extreme heat events [22]. A related and emerging question in geodemographics involves incorporating individual-level information into neighborhood typologies to provide more targeted support for resource allocation and policy interventions [23]. We develop a novel neighborhood characterization approach that combines each of these threads to produce a typology of neighborhoods throughout the Atlanta MSA based on individual-level social composition. Our approach enables assessment of the social impacts of climate stressors in Atlanta with respect to environmental justice and six EPA EJSCREEN risk factors (sensitive age groups, racial/ethnic minority status, linguistic isolation, poverty, and low economic mobility [educational attainment]).

The individual-oriented geodemographic classification for Atlanta relies on synthetic populations, a data product that fuses individual-level information from census microdata with population summary statistics to realistically approximate neighborhood social composition [24]. We generated 30 residential synthetic populations for the Atlanta MSA using the ORNL UrbanPop framework and data from the American Community Survey (ACS) 2015 - 2019 5-Year Estimates and the Public-Use Microdata File (PUMS). We then identified individual profiles (all unique combinations of EPA EJSCREEN indicators from the pooled PUMS files for Atlanta) and tabulated the block group synthetic populations by individual profile type. Final estimates of individual profiles by block group were taken as the median estimate across the 30 UrbanPop simulations.

We applied a method developed by Tuccillo [25] to compare block group synthetic populations and generate neighborhood cluster labels. Block group embeddedness scores were computed from a spectral decomposition of $C \times (1 + P)$, where C is a matrix of conceptual similarities among individual profiles and P is a matrix of similarities in size among individual profiles for that block group. The block group dissimilarity matrix was computed from the embeddedness scores and Ward hierarchical clustering to identify an appropriate number of clusters based on cluster separation (average silhouette width) and the quality of partitioning based on the proportion of inertia explained by the cluster labels (ratio of between-cluster sum of squares to total sum of squares).

We profiled the clusters based on the relative prevalence of individual profiles across member block groups by drawing 1,000 location-stratified samples of one individual each from each block group synthetic population. The selection probability of each individual profile is that individual profile’s proportion of the synthetic population. For organizational purposes, the individual profiles were arranged along an index based on a rank-1 embedding of the Jaccard dissimilarities among individual profiles using the multidimensional scaling (MDS) method. For each cluster, we performed unidimensional Gaussian kernel-density estimation individual profiles by index. The top 25% of modes by density were retained as cluster exemplars.

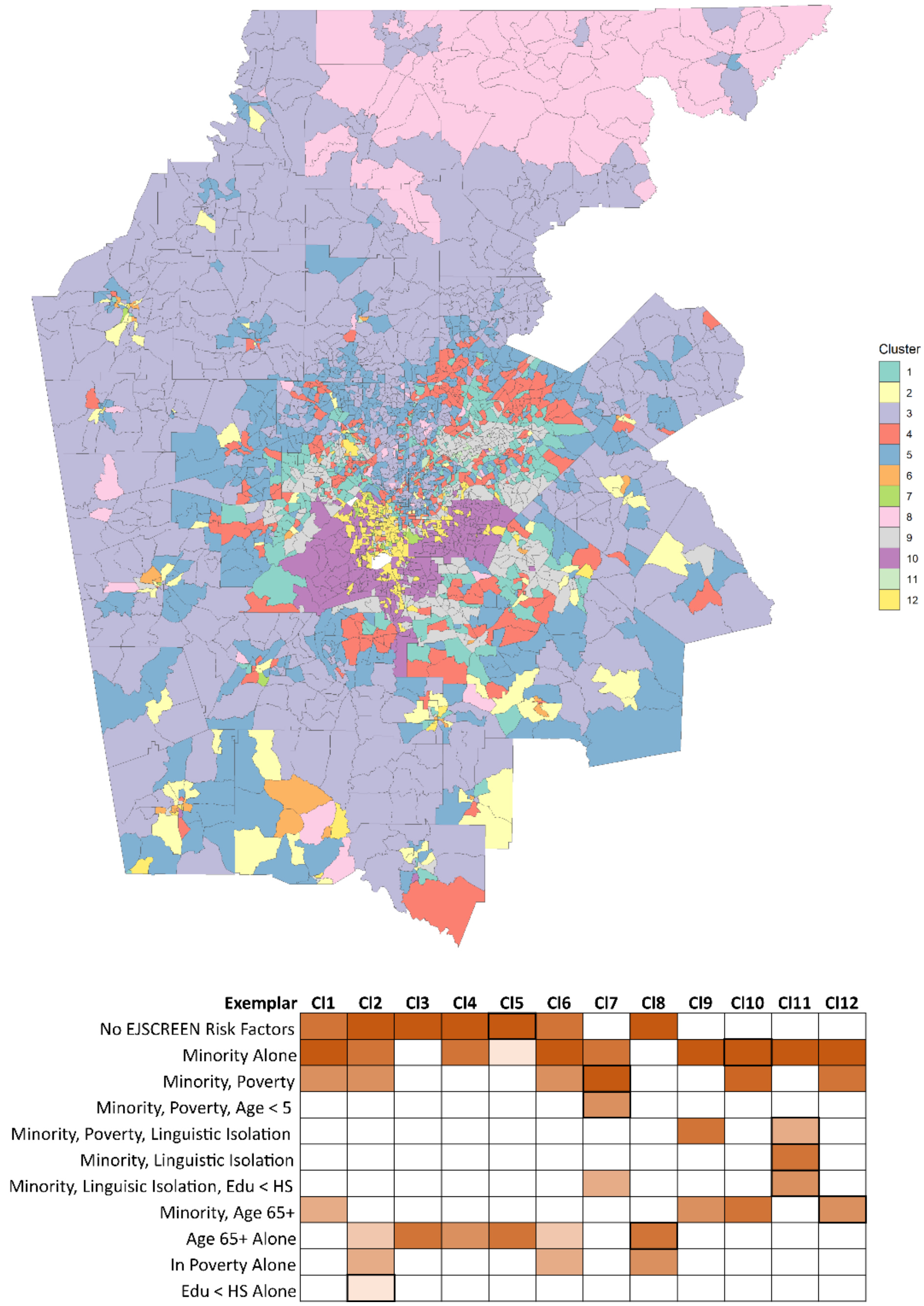

Figure 2. Overview of geodemographic clustering for Atlanta MSA.

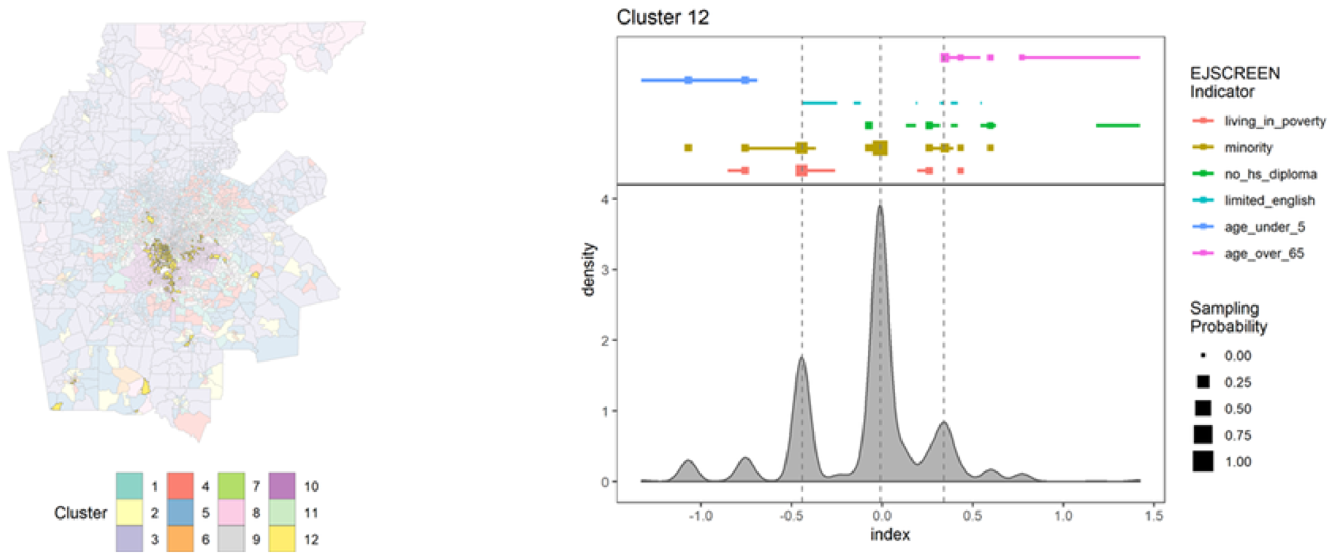

Figure 3– Example detailed profile for a single block group cluster (Cluster 12). The panel on the left shows the locations of member block groups within the Atlanta MSA.

Figure 2 provides an overview of the geodemographic typology for the Atlanta MSA, with profiles (bottom panel) characterizing the social mix within block groups belonging to each cluster. The cell shading in the profile plot represents the relative rank of the exemplar profile in the cluster, while the bolded panels denote exemplars that are often more prevalent within that cluster than in others. For example, Cluster 7 is strongly characterized by people with minority status and in poverty, including young children under the age of five, while a more central population characteristic in Cluster 11 block groups is minority status and linguistic isolation, including common interactions between linguistic isolation/poverty status and linguistic isolation/less than high school educational attainment.

Figure 3 provides a detailed profile for a single block group cluster (Cluster 12). The panel on the left shows the locations of member block groups within the Atlanta MSA. The right panel characterizes the social mix in block groups comprising the cluster with respect to individual attributes and exemplars. Each exemplar is represented by a distinct combination of EJSCREEN risk factors, denoted by the vertical line at its location on the x-axis. Cluster 12 exemplars shown in Figure 2 indicate that member block groups are typically represented by some combination of individuals characterized by 1) minority status alone, 2) minority status and poverty, and 3) minority status and advanced age (over 65).

3. Impacts by Climate Stressors

We use urban heat island (UHI) data [25] to understand how various neighborhoods are impacted by UHI and understand the differential impact on communities. Figure 5 displays the results of an exploratory analysis comparing the geodemographic block group clusters to daytime and nighttime UHI trajectories (land surface and ambient temperature difference) in the Atlanta MSA between 2003 - 2018. We observed general warming trends in the daytime UHI across most geodemographic block group clusters. Of the block group clusters experiencing generally steady increases in daytime UHI, two also experienced elevated nighttime UHI during the observation period:

- Cluster 2 (Exemplars: No EJSCREEN Risk Factors, Minority Alone, Minority/Poverty, Poverty Alone, Education less than High School Alone, Age 65+ Alone)
- Cluster 7 (Exemplars: Minority/Poverty, Minority/Poverty/Under Age 5, Minority Alone, Minority/Linguistic Isolation/Education less than High School).

Other clusters experienced generally steady increases in daytime UHI but more modest or fluctuating nighttime UHI:

- Cluster 11 (Exemplars: Minority Alone, Minority/Poverty, Minority/Linguistic Isolation, Minority/Poverty/Linguistic Isolation, Minority/Linguistic Isolation/Education less than High School)
- Cluster 6 (similar profile to Cluster 2 but with less frequent occurrence of people with Education less than High School alone).

Clusters largely located in peripheral areas of the Atlanta MSA (4, 8), appear to also have experienced overall increases in daytime/nighttime UHI over the observation period.

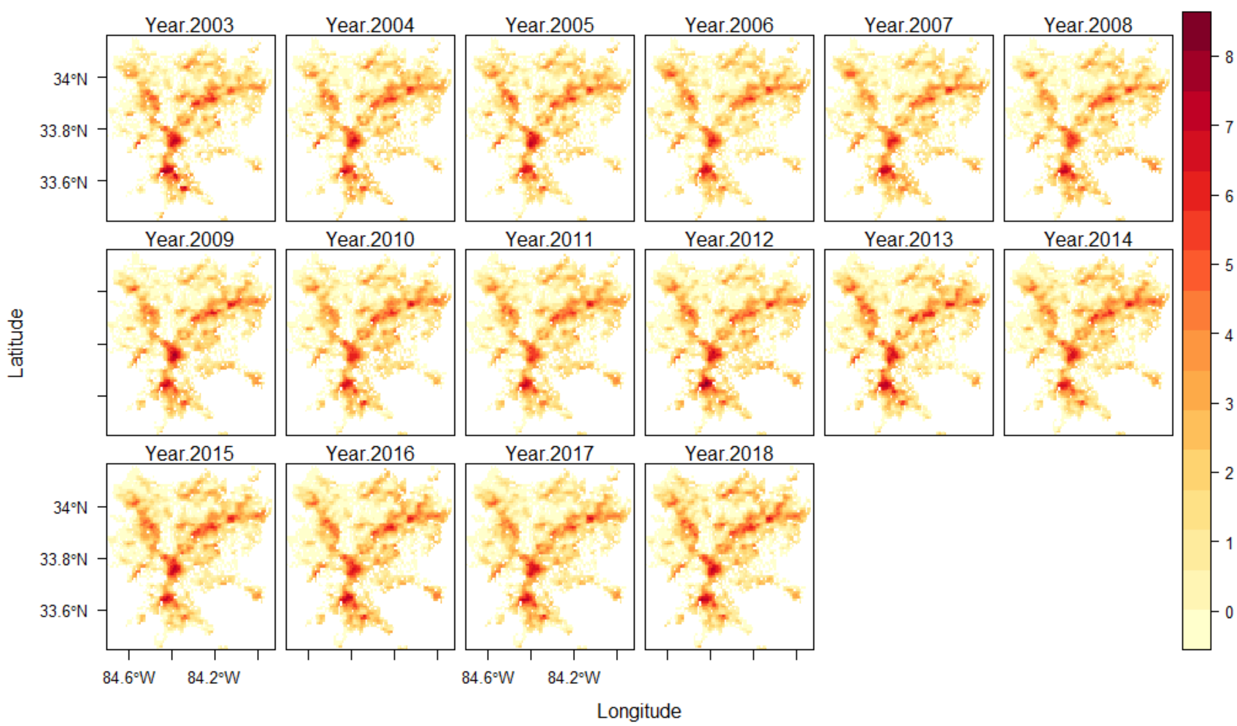

Figure 4- Summertime Urban Heat Island (UHI) temperature (℃) derived from MODIS data is shown for the Atlanta metropolitan area. Data source: https://yceo.yale.edu/research/global-surface-uhi-explorer.

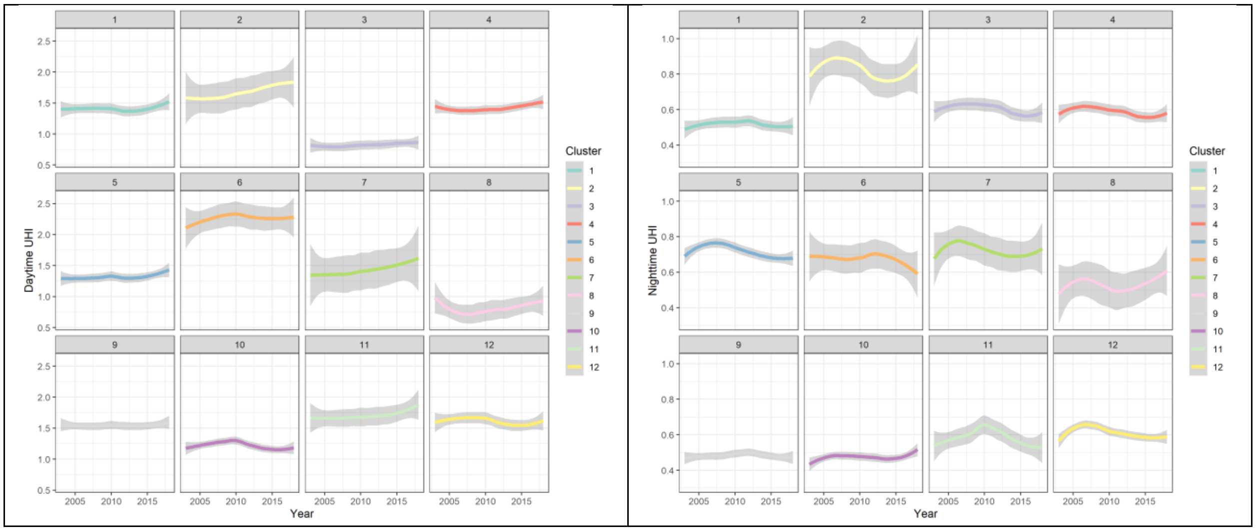

Figure 5. Smoothed conditional mean estimates of UHI (land surface and ambient temperature difference) by geodemographic block group cluster, 2003 - 2018.

Conclusion

We developed an initial framework for identifying 'neighborhoods-at-risk' using a data-centric approach. The approach is scaleable over space and time providing a capability which can be applied to future urban expansion. As cities grow and socio-demographic patterns change with expansion of suburban areas to urban and rural to suburban, it is critical to understand the consequences of climate change compounded by the impacts of urban expansion to ensure environmental justice across communities.

References

[1] Tessum, C. W., Paolella, D. A., Chambliss, S. E., Apte, J. S., Hill, J. D., & Marshall, J. D. (2021). PM2. 5 polluters disproportionately and systemically affect people of color in the United States. *Science Advances*, *7*(18), eabf4491.

[2] Mohai, P., & Saha, R. (2015). Which came first, people or pollution? A review of theory and evidence from longitudinal environmental justice studies. *Environmental Research Letters*, *10*(12), 125011.

[3] Tessum, C. W., Apte, J. S., Goodkind, A. L., Muller, N. Z., Mullins, K. A., Paolella, D. A., ... & Hill, J. D. (2019). Inequity in consumption of goods and services adds to racial–ethnic disparities in air pollution exposure. *Proceedings of the National Academy of Sciences*, *116*(13), 6001-6006.

[4] Simpson, N. P., Mach, K. J., Constable, A., Hess, J., Hogarth, R., Howden, M., ... & Trisos, C. H. (2021). A framework for complex climate change risk assessment. *One Earth*, *4*(4), 489-501.

[5] Dobson, J. E., Bright, E. A., Coleman, P. R., Durfee, R. C., & Worley, B. A. (2000). LandScan: a global population database for estimating populations at risk. *Photogrammetric engineering and remote sensing*, *66*(7), 849-857.

[6] Leyk, S., Nagle, N. N., & Buttenfield, B. P. (2013). Maximum entropy dasymetric modeling for demographic small area estimation. *Geographical Analysis*, *45*(3), 285-306.

[7] Diaz, D., & Moore, F. (2017). Quantifying the economic risks of climate change. *Nature Climate Change*, *7*(11), 774-782.

[8] Rufat, S. (2013). Spectroscopy of urban vulnerability. *Annals of the Association of American Geographers*, *103*(3), 505-525.

[9] Wood, N. J., Jones, J., Spielman, S., & Schmidtlein, M. C. (2015). Community clusters of tsunami vulnerability in the US Pacific Northwest. *Proceedings of the National Academy of Sciences*, *112*(17), 5354-5359.

[10] Wolf, T., & McGregor, G. (2013). The development of a heat wave vulnerability index for London, United Kingdom. *Weather and Climate Extremes*, *1*, 59-68.

[11] Smit, B., & Wandel, J. (2006). Adaptation, adaptive capacity and vulnerability. *Global environmental change*, *16*(3), 282-292.

[12] Fussell, E. (2015). The long-term recovery of New Orleans' population after Hurricane Katrina. *American Behavioral Scientist*, *59*(10), 1231-1245.

[13] Hoffman, J. S., Shandas, V., & Pendleton, N. (2020). The effects of historical housing policies on resident exposure to intra-urban heat: a study of 108 US urban areas. *Climate*, *8*(1), 12.

[14] Anderson, Meg, and Sean McMinn. "As Rising Heat Bakes U.S. Cities, The Poor Often Feel It Most." *NPR*, NPR, 3 Sept. 2019, www.npr.org/2019/09/03/754044732/as-rising-heat-bakes-u-s-cities-the-poor-often-feel-it-most.

[15] Cutter, S. L., Boruff, B. J., & Shirley, W. L. (2003). Social vulnerability to environmental hazards. *Social science quarterly*, *84*(2), 242-261.

[16] Cutter, S. L., & Finch, C. (2008). Temporal and spatial changes in social vulnerability to natural hazards. *Proceedings of the national academy of sciences*, *105*(7), 2301-2306.

[17] Flanagan, B. E., Gregory, E. W., Hallisey, E. J., Heitgerd, J. L., & Lewis, B. (2011). A social vulnerability index for disaster management. *Journal of homeland security and emergency management*, *8*(1).

[18] U.S. Environmental Protection Agency (EPA), 2019. EJSCREEN Technical Documentation.

[19] Singleton, A. D., & Longley, P. A. (2009). Geodemographics, visualisation, and social networks in applied geography. *Applied Geography*, *29*(3), 289-298.

[20] Gale, C. G., Singleton, A., Bates, A. G., & Longley, P. A. (2016). Creating the 2011 area classification for output areas (2011 OAC). *Journal of Spatial Information Science*, *12*, 1-27.

[21] Weatherburn, T., & Naud, D. (2011). Geodemographics and Environmental Justice in Montreal: Exploring Socioeconomic Position Through Geodemographic Segmentation. In *Mapping Environmental Issues in the City* (pp. 49-68). Springer, Berlin, Heidelberg.

[22] Tuccillo, J. V., & Buttenfield, B. P. (2016, September). Model-based clustering of social vulnerability to urban extreme heat events. In *The Annual International Conference on Geographic Information Science* (pp. 114-129). Springer, Cham.

[23] Burns, L., See, L., Heppenstall, A., & Birkin, M. (2018). Developing an individual-level geodemographic classification. *Applied Spatial Analysis and Policy*, *11*(3), 417-437.

[24] Harland, K., Heppenstall, A., Smith, D., & Birkin, M. H. (2012). Creating realistic synthetic populations at varying spatial scales: A comparative critique of population synthesis techniques. *Journal of Artificial Societies and Social Simulation*, *15*(1).

[25] Tuccillo, J. (2021). An Individual-Centered Approach for Geodemographic Classification. *GIScience 2021 Short Paper Proceedings*. https://doi.org/10.25436/E2H59M

[26] T. Chakraborty, X. Lee, "A simplified urban-extent algorithm to characterize surface urban heat islands on a global scale and examine vegetation control on their spatiotemporal variability", International Journal of Applied Earth Observation and Geoinformation. 74, 269-280, 2019.